Precise measurements of hot S-parameters of superconducting cavities: Experimental setup and error analysis

Anirban Krishna Bhattacharyya*, Volker Ziemann*, Tor Lofnes*, Han Li*, Roger Ruber*, Vitaliy Goryashko*

Ångströmlaboratoriet, Department of Physics and Astronomy, Uppsala University, Uppsala, Sweden

Abstract

Superconducting accelerating cavities used in modern particle accelerators change their intrinsic properties when excited to very high field levels close to the critical field where the superconductivity is affected. In this report we describe a test-bench and data analysis procedure to determine the so-called hot S-parameters from strongly driven cavities and use them to quantify the properties of the cavity at varying field levels. The method is based on analysing reflection coefficient for a large number of configurations in a self-excited loop setup and determining the cavity coupling coefficient $\kappa = Q_0/Q_{ext}$ as a function of cavity voltage to high accuracy. Since Q_{ext} is determined independently and is a constant, from the information of κ the Q-slope can be determined.

Keywords: superconducting cavity, Q-slope, hot S-parameters, Q-circle, self-excited loop

2010 MSC: 00-01, 99-00

1. Introduction

The modern accelerator facilities, like XFEL and ESS, which require large beam energy, rely on superconducting (SC) radiofrequency (RF) cavities to achieve their desired performance [1, 2]. The cavities are characterized in terms of scattering parameters (S-parameters) commonly used for the characterization of RF networks [3, 4]. In contrast to normal conducting RF cavities, SC

*Corresponding author

Email address: anirban.bhattacharyya@physics.uu.se (Anirban Krishna Bhattacharyya)

RF cavities change their characteristics, such as the quality factor, the surface resistance and frequency with the field excited in the cavity [5]. As a result, the S-parameters change as a function of the cavity field. The S-parameters of a system under test that are dependent on the state of the system are referred to as hot S-parameters [6]. Though the techniques for measuring hot S-parameters of traditional RF components such as RF amplifiers are well-developed [6], to our best knowledge the techniques for measuring hot S-parameters of SC cavities *operated at fields comparable to the critical field* are not established yet. One can only mention recent results on accurate measurements of S-parameters of SC cavities operated at *low-field* when the cavity parameters are practically independent of the cavity voltage [7]. In this paper we present the developed test bench and analyse its performance to measure the hot S-parameters of the prototype single spoke cavities for ESS at FREIA using the Horizontal Nugget for Operation of Superconducting Systems (HNOSS) cryostat [8].

SC cavities used in particle acceleration are immersed in a helium bath for maintaining a superconducting state under high RF fields. The cavity walls are made thin for good transfer of heat generated by the RF fields in the cavity to the bath. However, thin cavity walls make the cavities mechanically sensitive to fluctuations of the helium bath pressure as well as other mechanical vibrations [9]. The cavity changes its shape, which according to Slater's perturbation theorem [10] causes a change in the cavity frequency. The latter can be as large as a few hundreds of Hz though the cavity geometry only changes by some microns [11–13]. These fluctuations of the cavity frequency make a conventional measurement of the cavity S-parameters with a vector network analyser (VNA) impossible, since the cavity bandwidth is below 1 Hz and it moves out of tune by many orders of magnitude. Therefore, we operate the cavity as part of an oscillator built around it using a self-excited loop [14, 15]. This allows tracking of the cavity frequency and amplitude in a straight-forward way by eavesdropping on the signal propagating within the self-excited loop.

Recently, we proposed a novel method to accurately determine the Q-factor of a cavity as a function of voltage. A description of the method and some

results can be found in [16]. Here, we present the details of the test bench that allows high-precision measurements of hot S-parameters, which leads to highly accurate characterization of the cavity Q-slope.

This paper is organized in the following way. First we recapitulate the idea of the method [16] and then present our test setup followed by a description of the experiment preparation and the descripton of the data and error analysis. Finally we present the results and conclude.

2. The Q circle Method

Resonant modes of standing electromagnetic (EM) waves in cavities can be described by an equivalent forced oscillator model [16]. An EM wave not only enters the cavity through the power coupler but also leaks out through it forming a reflected wave. The reflection coefficient Γ, or S_{11} parameter, which quantifies the reflected wave is defined as the ratio of the reflected voltage to the incident one and is given by

$$\Gamma = \frac{\kappa - 1 + iQ_0\delta}{\kappa + 1 - iQ_0\delta} \tag{1}$$

where, $\kappa = \frac{Q_0}{Q_{ext}}$ is the coupling coefficient and

$$\begin{aligned} \delta &= \frac{\omega_c(t)}{\omega} - \frac{\omega}{\omega_c(t)} \\ &\approx \frac{Q_{ext} + Q_0}{Q_0 Q_{ext}} \tan(\theta_c) \end{aligned} \tag{2}$$

is the relative detuning of the cavity. Q_0 is the quality factor which qualifies the energy lost in a cavity, Q_{ext} is the quality factor which describes the energy lost through the power coupler, $\omega_c(t)$ is the instantaneous cavity frequency, ω is the excitation signal frequency, and θ_c is the phase shift across the cavity [16]. In general the cavity quality factor Q_0 depends on the cavity voltage [5]. Therefore, the coupling coefficient κ depends on the cavity voltage V as well.

Rewriting equation (1) to separate real and imaginary parts we find

$$i\Gamma'' + \Gamma' + 1 = -\frac{2iQ_0}{Q_0(Q_{ext}\delta - i) - iQ_{ext}}, \tag{3}$$

which can be further simplified using equation (2) and eliminating the phase shift across the cavity θ_c, to obtain

$$\left(\Gamma' + \frac{1}{1+\kappa}\right)^2 + \Gamma''^2 = \left(\frac{\kappa}{1+\kappa}\right)^2 \tag{4}$$

which is the equation of a circle with centre at $(-\frac{1}{1+\kappa}, 0)$ and radius of $r = \frac{\kappa}{1+\kappa}$. Then the coupling coefficient can be calculated using

$$\kappa = \frac{1}{\frac{1}{r} - 1}. \tag{5}$$

The circle traced out by the reflection coefficient on the complex plane of the Smith-Chart is termed as the Q circle. This method however cannot be used if κ changes significantly when changing the cavity voltage V, which is the case for superconducting cavities. The dependence of κ on V causes the variation of the reflection coefficient to deviate from a circle (see Figure 1) and the method needs to be modified. For fixed cavity voltage, κ is constant and the reflection

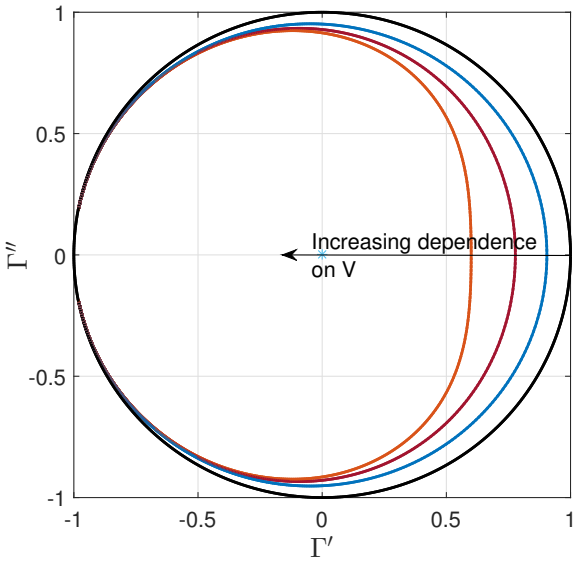

Figure 1: Variation of Q circle with increased dependence on cavity voltage V. Since the reflection coefficient becomes a function of the cavity voltage, conventional methods of measurement of reflection coefficient fail in such cases.

coefficient traces a circle, while for varying cavity voltage V it traces a surface in the 3-D κ - Γ space which we call Q-surface as shown in Figure 2. This means that when we do measurements and observe the reflection coefficient, we observe the projection of a path on the Q-surface on the Γ'-Γ'' plane. In order to assemble circles we simultaneously need to estimate the cavity voltage from experiments. In the next section we present the experimental set up to obtain the voltage dependent κ values and eventually Q_0.

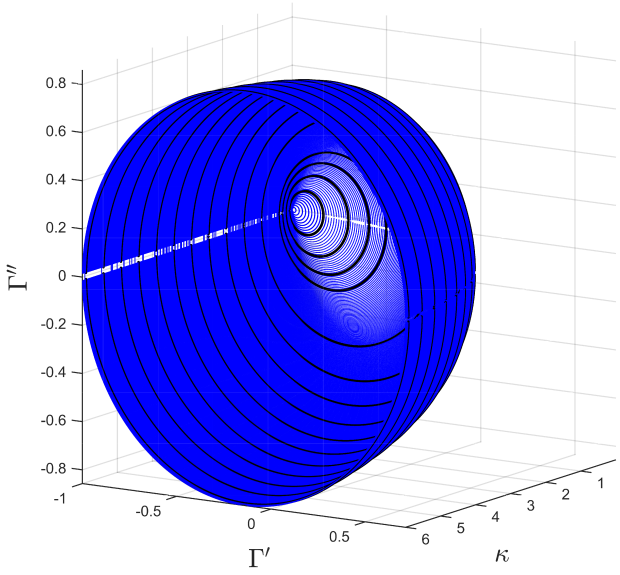

Figure 2: The variation of reflection coefficient with κ. The Q-surface is shown in the figure. Measurement of the reflection coefficient of a super conducting cavity is the locus of points on this surface and as a result it might not remain a circle anymore.

3. The test bench: Self-excited Loop

The experimental bench for the RF measurements is a self excited loop [14], which is an oscillator built around the cavity, with the schematic shown in Fig. 3. The loop consists of the SC cavity, amplifiers and limiters and the digital loop delay. The vector network analyser and the directional couplers are

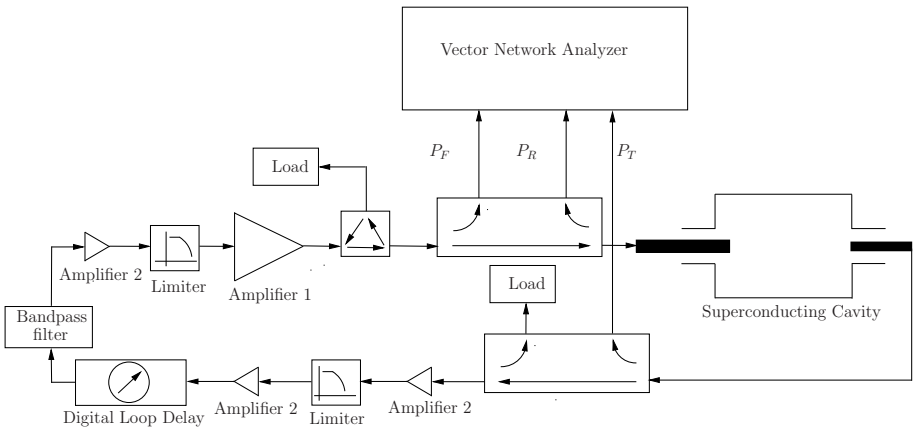

Figure 3: Setup for self excited loop based measurement of Q circle. The vector network analyser working as a superheterodyne receiver, tuned to the cavity bandwidth, measures the forward, reflected and transmitted signals to and from the cavity under test. The signal picked up from the cavity is sent through amplifier-limiter-amplifier combination to mantain high signal-to-noise ratio and then delayed by means of the digital loop delay. Variation of the delay, changes the phase shift across the cavity and scans the reflection coefficient as a function of cavity phase. This changes the loop resonance frequency, which might differ from the cavity resonance frequency and thus result in variation of the forward, reflected and transmitted signals. Using this data the Q surface can be constructed.

added for diagnostics. The loop signal frequency is determined by the resonance frequency of the cavity and the phase across the loop. The cavity being narrow band only allows frequencies within the bandwidth to pass, which can then drive the amplifier back and thus keep the loop alive. The loop, on the other hand only allows those frequencies to survive for which the total change in phase across the loop is a multiple of 2π.

Starting immediately after the cavity we have a directional coupler that directs part of the transmitted signal to the VNA but most of the power is passed through a sequence of amplifier-limiter-amplifier. This configuration allows the limiter to operate in its preferred range and thus provides good signal-to-noise ratio while protecting the delicate electronics of the digital loop delay. Subsequently the signal is passed through a sequence of amplifier, limiter, and power amplifier before a directional coupler directs a small fraction of the forward and

reflected power signals to the VNA. The dominant part of the signal is directed to the cavity.

3.1. Amplifiers and limiters

The power amplifier, labelled Amplifier 1 in Fig.3 excites the cavity with a power of up to 100 W [17]. The smaller amplifiers labelled amplifier 2 are low-noise amplifiers with a noise figure of 0.4 dB at around 400MHz [18, 19]. The limiter limits the signal at 0 dBm [20].

3.2. Cables and vector network analyser (VNA)

The cavity in the bunker and the measurement instruments in the control room are separated by cables 25m long, which cause signal attenuation and phase delay. While the effect of the phase delay only introduces a rotation of the Q-circle the attenuation affects the diameter of the circle and thus needs to be corrected.

We determine the cable attenuation by tuning the cavity off its resonance such that all power is reflected and record the forward and reflected power in the control room with a 4-port VNA that we calibrated with a 4-port Electronic calibration kit. The expected error bars for amplitude and phase are ± 0.06dB and $\pm 0.4^{\circ}$, respectively [21].

The cavity in a superconducting state, has a very small bandwidth of a few Hertz. In order to measure the S-parameters of the cables a signal generator is used to send power to the cavity, and the VNA measures the power (forward and reflected) at the point of Q circle measurement. The power and frequency of the RF signal sent by the generator is varied and the measurement is carried out. The frequency of the signal is kept outside cavity resonance and bandwidth so that all the power is reflected back from the cavity. From the measurements, the cable attenuation is determined to be 3.9 ± 0.02 dB.

3.3. Digital Loop delay

We introduce the phase delay that determines the operating frequency of the self-excited loop with a digital loop delay or phase shifter. Our implementation

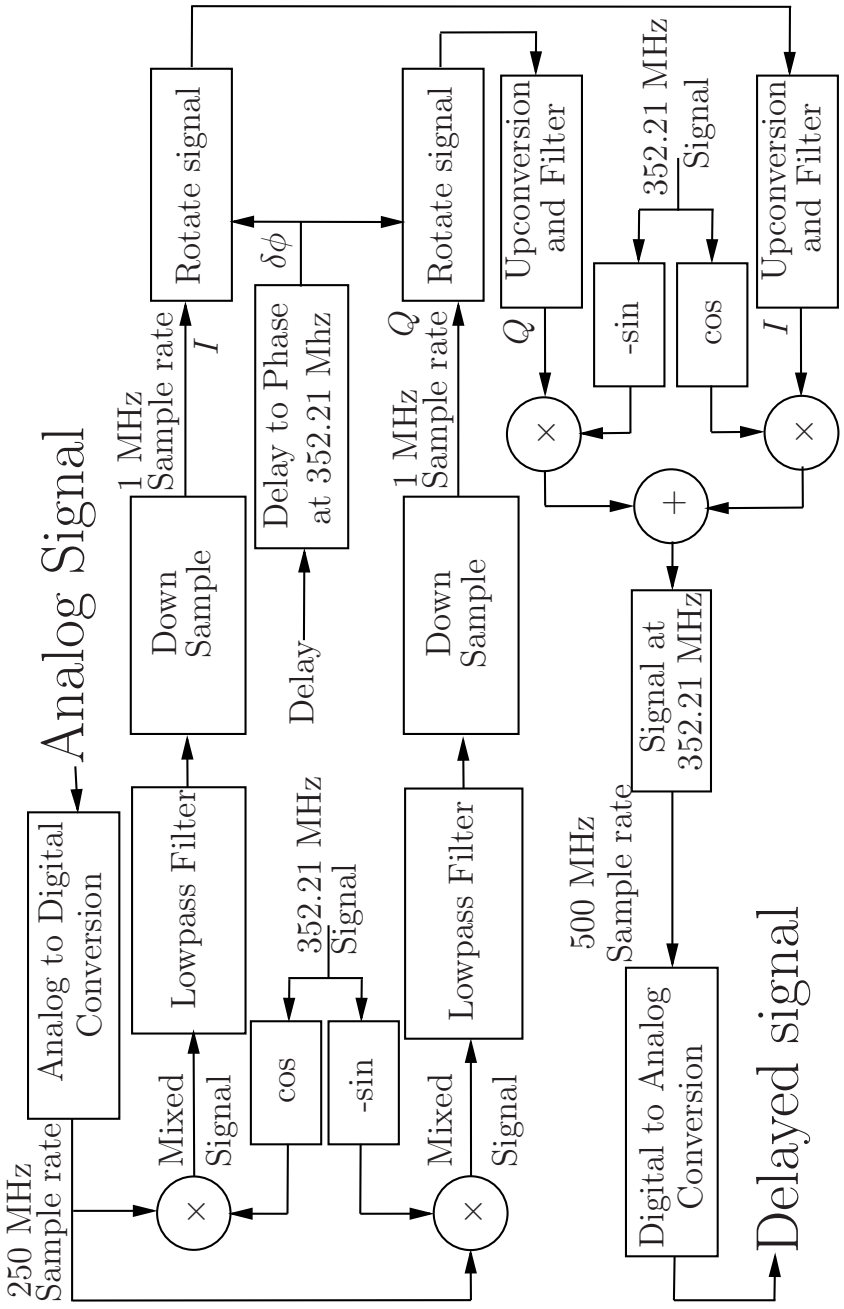

Figure 4: Digital down-conversion scheme for loop delay introduction.

uses the super-heterodyne principle for radio transceivers. The dominant mode of the cavity is 352.21MHz. The first step is to convert the analog loop signal to a digital one. This is achieved using an IF transceiver with AC-coupled option with Dual 14-bit, 250 MS/s inputs housed in a PXIe chassis [22]. Since the sampling rate is lower than that required by Nyquist criterion, the technique used here is that of under-sampling. However, since the signal of interest is the only signal present in the loop, this causes no problem downstream if proper filtering and frequency scaling is used. Under-sampling implies that in the digital system, 352.21MHz appears at around 102.21MHz. Once digitized, the signal is mixed with a digital signal of 102.21MHz and then sequentially low-pass filtered and decimated to reduce the sampling rate from 250 MS/s to 1 MS/s. This is implemented in software using an NI FlexRIO FPGA module programmed using LabVIEW.

The time delay or phase shift algorithm on the FPGA is based on rotating the in-phase (I) and quadrature (Q) component of the signal in baseband according to

$$\begin{aligned} I_r &= I\cos(\delta\phi) - Q\sin(\delta\phi) \\ Q_r &= I\sin(\delta\phi) + Q\cos(\delta\phi). \end{aligned} \tag{6}$$

where we converted the time delay δt to a phase delay by $\delta\phi = \omega\delta t$, I_r and Q_r are the phase-shifted signals. The signal is then digitally mixed with the sine and cosine components of the digital local oscillator and converted back to analog in a Dual 16 bit, 500 MS/s digital-to-analog converter that is part of the IF transceiver.

The output is thus under-sampled as well which means that there is an output signal not only at 352.21 MHz but also at the mirror frequency 147.79 MHz (500 MHz - 352.21 MHz). The 147.79 MHz component of the signal is removed by three VAD 1172 circulators [23] connected in series, acting as a band-pass filter around 352.21 MHz. After that the signal is sent to the power amplifier.

4. Experimental preparation with the Superconducting Cavity

The cavity under test is a double spoke cavity developed at IPN Orsay to be used in the European spallation source in Lund, Sweden [24]. The cavity was designed and went through initial tests at IPNO, Orsay.

4.1. Cool down

The cavities are made of niobium which is super-conducting below 9.2 K. The cavities have a working temperature of 2 K, which is achieved using liquid Helium. The cavities are housed in the HNOSS cryostat [8], as shown in Fig. 5, and are cooled by liquid Helium systems. The cool down rates can be controlled depending upon the need of the experiments. For the measurements of cavity quality factor using the self excited loop, cooling is done at the maximum rate possible at FREIA, which gives the best results for attaining super conducting state all across the cavity while avoiding hotspots. The cavity is cooled from 200K to around 10 K in around 15 minutes as shown in Fig 6.

4.2. Conditioning

Before the signal from the cavity can be used for the self excited loop, the cavity needs to be conditioned so that any surface impurities are burnt away and the resultant residues extracted by the vacuum system [25]. This process of conditioning has to be carried out at the maximum power that can be handled by the cavity, and results in considerable x-ray emission which is recorded by x-ray detectors placed in the bunker around the cavity (Figure 7). Such emission can happen at RF frequencies other than cavity resonance and this can be effectively carried out by changing the loop delay and setting the frequency of the self excited loop (this effect can be seen from Point 1 to Point 2 in Figure 7). Once the detected x-ray emission dies out the signal from the cavity can be used for Q circle measurements.

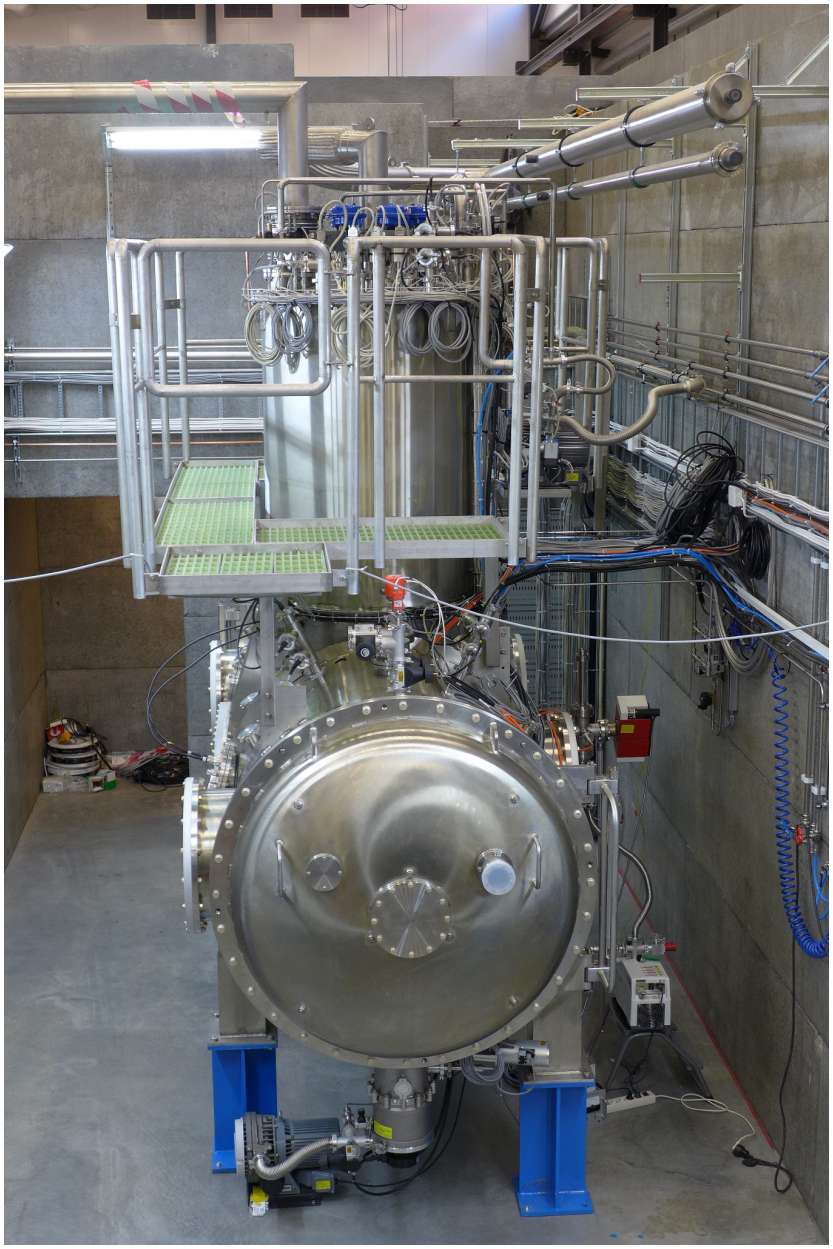

Figure 5: The HNOSS cryostat housing the cavity in the bunker. It is fed with liquid Helium and liquid Nitrogen systems to cool down and achieve superconducting state.

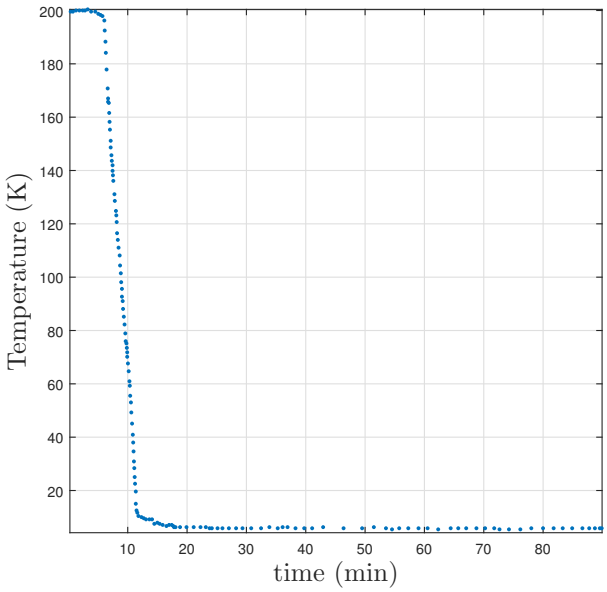

Figure 6: Cool down rate of the cavity. Cool down till 10 K is done fast in around 12 minutes.

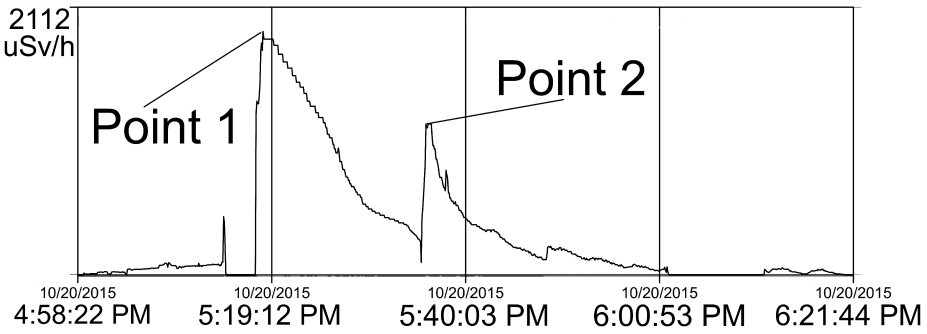

Figure 7: Radiation spectrum during conditioning of cavity. Point 1 and Point 2 depict X-ray emission due to excitation of frequencies from impurities and surface roughness.

5. Determination of κ or Q_0 from measured data

The measured reflection coefficients after the correction for the cable attenuation are shown in Fig. 8. Comparing these measurements to Fig. 1 we see a nature similar to the theoretical discussion in section 2 for cavity voltage V

dependent Q_0 or κ.

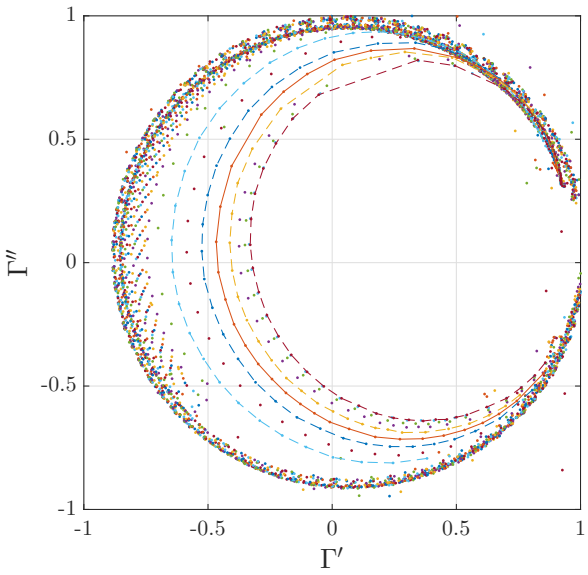

Figure 8: Reflection coefficient measured after cable compensation. The curves are not circles and this points to the fact that the cavity quality factor is dependent on cavity voltage.

Now, if we also plot the variation of V along with the complex reflection coefficient, then we see the Q surface that we introduced in section 2 and extract Q circles from there. We can now use equation (5) to estimate κ.

5.1. Formation of Q circles

There are two loop parameters which we can change in the self-excited loop, the loop gain and the loop delay. While, the loop gain determines the maximum possible power input to the cavity on tune, the loop delay determines the signal frequency. However, by changing the loop delay we move the loop frequency across the very narrow cavity resonance and thus affect the power accepted by the cavity. Hence the loop delay changes both frequency and voltage level in the cavity. Repeating the delay-scan at different amplifier gain settings permits recording the cavity voltage and the reflection coefficient $\Gamma = \Gamma' + i\Gamma''$ which

permits us to assemble data points that cover a very large fraction of the Q-surface as shown in Fig. 2. This operation of Q-surface scan takes about 24-hours, depending upon the density of points.

To extract Q circles from the 3-D plots we bin the data along the V axis and fit circles to the points in each bin. For the data obtained from the experiments the minimum and maximum variation of voltage bins is from 0.005 MV to 0.1 MV. After the binning the Q circle variation can be displayed with respect to V as shown in Fig. 9.

5.2. Fitting Q circles and error analysis

Equation (4) can be rewritten in the following form

$$\left(\Gamma' + \frac{1}{\kappa+1}\right)^2 + \Gamma''^2 = \left(1 - \frac{1}{\kappa+1}\right)^2 \tag{7}$$

where Γ' and Γ'' are the real and imaginary part of the complex reflection coefficient or the S_{11} parameter. Expanding the squares and collecting terms results in

$$1 - \Gamma'^2 - \Gamma''^2 = \frac{2}{\kappa+1}\left(1 + \Gamma'\right) \ . \tag{8}$$

This equation can be cast into the form of a least square fit where each measurement is labeled by integer n

$$\begin{pmatrix} \vdots \\ 1 - \Gamma'^2_n - \Gamma''^2_n \\ \vdots \end{pmatrix} = \begin{pmatrix} \vdots \\ 2\left(1 + \Gamma'_n\right) \\ \vdots \end{pmatrix} \frac{1}{\kappa+1}. \tag{9}$$

This is of the canonical form of a least squares fit $y = Ax$ for the unknown $x = 1/(\kappa+1)$ where y is the vector on the left hand side of the previous equation and the matrix A the vector on the right hand side. Ignoring any error bars this system can be solved in the least square sense by $x = (A^tA)^{-1}A^ty$ which, if written in component form, results in

$$\frac{1}{\kappa+1} = \frac{\sum_n (1+\Gamma'_n)(1-\Gamma'^2_n - \Gamma''^2_n)}{2\sum_n \left(1+\Gamma'_n\right)^2} \tag{10}$$

which can be trivially solved for κ.

In order to assess the error bars of the measurements of κ we introduce the parameter Z_n which ideally should be 0 in each line of eq. 9. This gives us

$$0 = Z_n = 1 - \Gamma_n'^2 - \Gamma_n''^2 - \frac{2}{\kappa+1}\left(1+\Gamma_n'\right) \tag{11}$$

and we introduce the modulus Γ_n and phase ϕ_n of the reflection coefficient Γ_n as

$$\Gamma_n' = \Gamma_n \cos\phi_n \qquad \text{and} \qquad \Gamma_n'' = \Gamma_n \sin\phi_n \tag{12}$$

such that we can write

$$Z_n = 1 - \Gamma_n^2 - \frac{2}{\kappa+1}\left(1+\Gamma_n\cos\phi_n\right) \tag{13}$$

and any error bars in Γ_n or ϕ_n will spoil the zero Z_n, which we then interpret that as the error bar for that equation. Using normal error propagation we need to calculate the partial derivatives of Z_n with respect to Γ_n and ϕ_n and find

$$\frac{\partial Z_n}{\partial \Gamma_n} = -2\Gamma_n - \frac{2}{\kappa+1}\cos\phi_n \qquad \text{and} \qquad \frac{\partial Z_n}{\partial \phi_n} = \frac{2\Gamma_n}{\kappa+1}\sin\phi_n \tag{14}$$

such that we arrive at the error bar for Z_n to assign to each measurement as

$$\begin{aligned} \sigma^2(Z_n) &= \left|\frac{\partial Z_n}{\partial \Gamma_n}\right|^2 \sigma^2(\Gamma) + \left|\frac{\partial Z_n}{\partial \phi_n}\right|^2 \sigma^2(\phi) \\ &= \left(2\Gamma_n + \frac{2}{\kappa+1}\cos\phi_n\right)^2 \sigma^2(\Gamma) + \left(\frac{2\Gamma_n}{\kappa+1}\sin\phi_n\right)^2 \sigma^2(\phi) \end{aligned} \tag{15}$$

where $\sigma(\Gamma)$ is the error in the measurement of the magnitude of the reflection coefficient and $\sigma(\phi)$ in the phase measurement.

We organize the error bars of each measurement point n in a diagonal matrix W which has the entries $\sigma(Z_n)$ on the diagonal and zeros elsewhere

$$W = \mathrm{diag}\left(\frac{1}{\sigma(Z_1)}, \ldots, \frac{1}{\sigma(Z_n)}, \ldots\right) . \tag{16}$$

These measurement errors can be incorporated in the data analysis by left-multiplying eq. 9 by W. This gives each measurement a weight inversely proportional to its measurement error bar. Redoing the above analysis we obtain for the fit result

$$\frac{1}{\kappa+1} = (A^t W^2 A)^{-1} A^t W^2 y. \tag{17}$$

As a result of the normal least square fit error analysis we also obtain the covariance matrix of the fit result $x = 1/(\kappa + 1)$ as

$$C_{xx} = (A^t W^2 A)^{-1} \quad \text{where} \quad x = \frac{1}{\kappa + 1} \; . \tag{18}$$

The error bar for κ can be found from that of x by inverting the equation relating x and κ with the result $\kappa = (1 - x)/x$ and since the covariance matrix propagates with the Jacobi matrix J we first calculate

$$J = \frac{\partial \kappa}{\partial x} = -\frac{1}{x^2} = -(\kappa + 1)^2 \tag{19}$$

and for the error bar $\sigma(\kappa)$ of the sought variable κ we thus get

$$\begin{aligned} \sigma(\kappa) &= \sqrt{J C_{xx} J^t} \\ &= (\kappa + 1)^2 \sqrt{C_{xx}} \\ &= (\kappa + 1)^2 \sqrt{(A^t W^2 A)^{-1}}. \end{aligned} \tag{20}$$

The fitted circles and their corresponding centres can be seen from Fig. 9. The process of fitting the Q-circles using equations (4) and (5) also calculates the coupling coefficient, κ along with its error estimate (using equation (20)), which is shown in Fig. 10.

The self-excited loop makes the method immune to multipacting near the connectors inside the cavity and any variation of the Helium pressure, while the order of magnitude reduction in error estimates has revealed fine features of change of cavity κ with cavity voltage V which are not visible in the single point measurements. Since κ and Q_0 are linearly related this also shows the variation of Q_0 with cavity field, which is the Q-slope. The sharp peaks and wiggles in the variation of κ or Q_0 may thus point some behaviour of superconductivity to low electromagnetic fields, a phenomenon not very well understood and provides a means of further investigation of the same. This can be achieved by repeating the experiments with better observation of all experimental parameters.

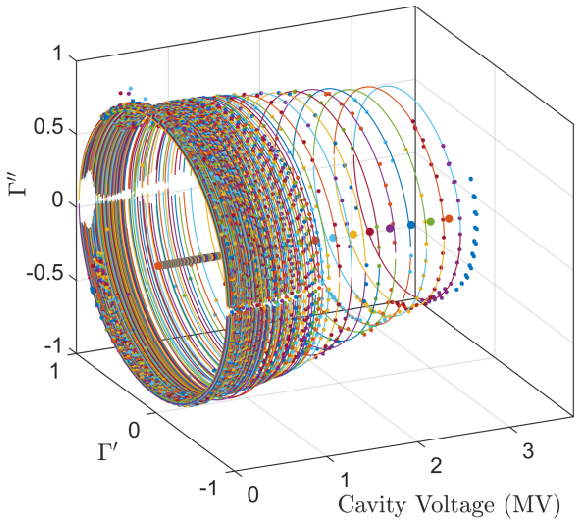

Figure 9: The reflection coefficient measurements are grouped by cavity voltage to obtain variation of Q-circle with accelerating voltage.

6. Conclusion

In this paper we present a procedure which allows characterisation of superconducting cavities from low to high field gradients with high accuracy. The test bench presented allows a large amount of measurements to be done in an automated procedure. The data are effectively analysed, and the coupling coefficient $\kappa = \frac{Q_0}{Q_{ext}}$ estimated to high accuracy from the overdetermined data set which reveals fine details of quality factor variation with accelerating gradient (high-field and low-field Q-slopes). This can then be used to investigate the effect of cool down rates of the cavities or any phenomena related to low-field superconductivity.

[1] S. Peggs, et al, Technical design report, Tech. Rep. ESS-2013-001, European Spallation Source (April 2013).

[2] M. Altarelli, et al, The european x-ray free-electron laser technical design report, Tech. rep., DESY (July 2007).

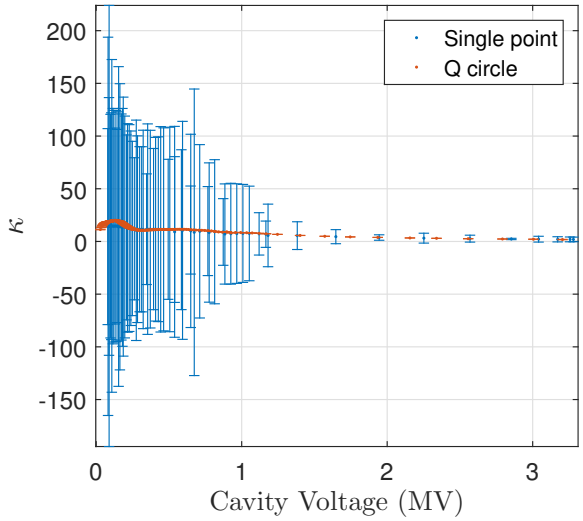

Figure 10: Variation of coupling coefficient, κ, with cavity voltage, V. The plot displays κ variation from both traditional single point measurements and the proposed technique. The accuracy of the proposed method cannot be obtained from single point measurement as was pointed out in [16]. The wiggles in the variation obtained from proposed method at low fields point to some characteristics of the cavity which are of interest for further studies. The large error in single point measurements is estimated using [16].

[3] Agilent Technologies, Agilent AN 154 S-Parameter Design (June 2006).
URL `http://cp.literature.agilent.com/litweb/pdf/5952-1087.pdf`

[4] D. M. Pozar, Microwave Engineering, 4th Edition, no. 978-0-470-63155-3, John Wiley and Sons, Inc., Weinheim, Germany, 2011.

[5] H. Padamsee, J. Knobloch, T. Hays, RF Superconductivity for Accelerators, 2nd Edition, John Wiley and Sons, Inc., Weinheim, Germany, 2008.

[6] D. Dancila, A. Eriksson, V. A. Goryashko, L. Haapala, R. Ruber, A. Rydberg, R. Wedberg, R. Yogi, V. Ziemann, Solid-state amplifier development at freia, in: C. Petit-Jean-Genaz, G. Arduini, P. Michel, V. R. Schaa (Eds.), IPAC2014: Proceedings of the 5th International Particle Accelerator Conference, Dresden, Germany, 2014, pp. 2282 – 2284.

[7] G. Cataldo, E. J. Wollack, E. M. Barrentine, A. D. Brown, S. H. Moseley, U. Kongpop, Analysis and calibration techniques for superconducting resonators, Review of Scientific Instruments 86 (1) (2015) 013103–1 – 013103–11. doi:10.1063/1.4904972.

[8] R. S. Kern, T. Ekelf, K. Gajewski, L. Hermansson, R. Ruber, V. Ziemann, P. Bujard, N. Chevalier, T. Junquera, J.-P. Thermeau, The hnoss horizontal cryostat and the helium liquefaction plant at freia, in: C. Petit-Jean-Genaz, G. Arduini, P. Michel, V. R. Schaa (Eds.), Proceedings of IPAC2014, Dresden, Germany, 2014.

[9] P. Petersan, S. Anlage, Measurement of resonant frequency and quality factor of microwave resonators: Comparison of methods, Journal of Applied Physics 84 (1998) 3392 – 3402.

[10] T. P. Wangler, RF Linear Accelerators, 2nd Edition, no. 978-3-527-40680-7, Wiley-VCH, Weinheim, Germany, 2011.

[11] J. Delayen, Ponderomotive instabilities and microphonics - a tutorial, Physica C: Superconductivity 441 (1 - 2) (2006) 1 – 6.

[12] M. Liepe, S. Belomestnykh, Microphonics detuning in the 500 mhz superconducting cesr cavities, in: J. Chew, P. Lucas, S. Webber (Eds.), Proceedings of the 2003 Particle Accelerator Conference, Portland, Oregon U.S.A, 2003, pp. 1326 – 1328.

[13] J. R. Delayen, G. K. Davis, Piezoelectric tuner compensation of lorentz detuning in superconducting cavities, in: Proceedings of the 11th Workshop on RF Superconductivity, Travemünde/Lübeck, Germany, 2003, pp. 665 – 668.

[14] M. Doleans, Studies in reduced-beta elliptical superconducting cavities, Phd thesis, Physique et Technologie des Grands-Instruments (September 2003).

[15] J. R. Delayen, Phase and amplitude stabilization of superconducting resonators, Ph.D. thesis, California Institute of Technology (August 1977).

[16] V. A. Goryashko, A. K. Bhattacharyya, H. Li, D. Dancila, R. Ruber, A method for high-precision characterization of the q-slope of superconducting rf cavities, Microwave Theory and Techniques IEEE Transactions on PP (99) (2016) 1 – 8. doi:10.1109/TMTT.2016.2605671.

[17] Mini-Circuits, Brooklyn, New York, Coaxial High Power Amplifier ZHL-100W-52+, d Edition.

[18] Mini-Circuits, Brooklyn, New York, Coaxial Low Noise Amplifier ZX60-P103LN+, a Edition.

[19] Modelithics, Mini-Circuits, Understanding Noise Parameter Measurements, b Edition (April 2015).

[20] Mini-Circuits, Brooklyn, New York, Coaxial Limiter ZFLM-252-1WL+, rev. a Edition.

[21] Keysight Technologies, http://literature.cdn.keysight.com/litweb/pdf/N5221-90001.pdf?id=2080065, Keysight 2-Port and 4-Port PNA Network Analyzer, data Sheet and Technical Specifications.

[22] National Instruments, NI 5782R User Manual and Specifications, ni.com.

[23] http://www.valvo.com/index.html.

[24] G. Olry, J.-L. Biarrotte, S. Blivet, S. Bousson, C. Joly, T. Junquera, J. Lesrel, A. Mueller, H. Saugnac, P. Szott, E. Zaplatin, Development of spoke cavities for the eurisol and eurotrans projects, Physica C: Superconductivity 441 (1 - 2) (2006) 201 – 204. doi:10.1016/j.physc.2006.03.116.

[25] H. Padamsee, RF Superconductivity: Volume II: Science, Technology and Applications, John Wiley and Sons, Inc., Weinheim, Germany, 2009.